First principles calculations of pentaheptite graphene and boronitrene derivatives

M. P. Molepo,[1,*] R. E. Mapasha,[1] K. O. Obodo,[1] and N. Chetty[1,2]

[1]*Department of Physics, University of Pretoria, Pretoria 0002, South Africa*
[2]*National Institute for Theoretical Physics, Johannesburg, 2000, South Africa*
**Email: Mahlaga.Molepo@up.ac.za Telephone: +27 (0)12 420 3502 Fax: +27 (0)12 362 5288*

(Dated: June 2, 2014)

We perform first principles density functional calculations to study the stability, structural and electronic properties of pentaheptite graphene and boronitrene derivatives. These systems are comprised of an infinite array of symmetrically paired pentagon and heptagon rings created by applying the Stone Wales transformation over infinite mono-layer graphene and boronitrene. Using the generalized gradient approximation (GGA) and the projector augmented wave (PAW) method, we predict that pentaheptite graphene is metallic and metastable with energy of 0.24 eV/atom above pristine graphene. We deduce that pentaheptite boronitrene is less stable due to the formation of unfavourable B-B and N-N bonds. Our results reveal a significant reduction in the electronic band gap for pentaheptite boronitrene in comparison to pristine boronitrene. Furthermore, we demonstrate that the adsorption of atomic hydrogen on pentaheptite graphene stabilizes the structure and opens a wide band gap of 3.78 eV.

Keywords: Pentaheptite; Stone Wales defects; Hydrogenation

I. INTRODUCTION

The experimental realization[1] of graphene has re-ignited a huge interest in the research of carbon-based materials. Graphene, which is a flat two-dimensional monolayer of covalently bonded carbon atoms arranged in a honeycomb lattice has unique electronic properties. It is well known that pristine graphene is a zero band-gap semi-metal. Its electronic structure exhibits a linear energy-dispersion relation near the Dirac point, with relativistic massless Dirac fermions being the charge carriers.[2,3] This special feature gives rise to various interesting properties including high carrier mobility,[4] which could be exploited for applications in high-performance graphene-based electronic devices. However, the absence of a band gap in pristine graphene is a limiting feature for applications in solid state electronic devices. On the other hand, monolayer hexagonal boron nitride (*h*-BN, also known as boronitrene, *cf.* Ref. 5) which is isostructural with graphene with nearly the same lattice parameter, has been synthesized and found to be a wide band gap semiconductor.[6]

Various approaches have been considered to alter the electronic structure of graphene so as to open a controllable band gap. These include chemical functionalization[7–15] as well as incorporating localized and extended defects.[16–23] Concerning the former, first principles electronic structure calculations and experiments have reported that graphene can be transformed into an insulating sheet, named graphane,[15] by complete hydrogenation. Graphane has been recently synthesized by Elias *et al.*,[9] following initial predictions by Sofo *et al.*[15] Quantum confinement effects have also shown the possibilities of band gap engineering, as in graphene nanoribbons[24–27] and nanomeshes[28] passivated with hydrogen. However, the resulting electronic properties are strongly dependent on the type of edge termination.

Among the possible intrinsic defects considered in graphene, Stone-Wales (SW) defects[29] are the most prevalent, as in other carbon nanostructures.[30–33] SW defects are formed by a 90° rotation of a carbon dimer with respect to the midpoint of the bond such that four hexagonal rings are transformed into pairs of pentagon (R_5) and heptagon (R_7) rings. Previous studies of SW patterned defects have consistently predicted metallic allotropes of graphene,[17,23] suggesting that their local structural distortions are not appropriate for opening an electronic band gap. Modification of a graphene monolayer into an infite array of SW defects[35,37] is expected to yield interesting electronic properties in comparison to its semimetalic behavior. This structure, so-called pentaheptite graphene was theoretically proposed by Crespi *et al.*, (Ref. 35) well before the experimental realization of graphene. Using a tight-binding total energy method, this system was predicted to be a covalent metal with a density of states at the Fermi level of 0.1 states per eV per atom.

Recently, first principles calculations have been used to investigate the adsorption of atomic hydrogen (H) on a single SW defected graphene substrate.[39] It was found that carbon atoms on the SW defect serve as energetically favorable "traps" for H adsorption suggesting that the electronic properties could be substantially changed by inclusion of H atoms into SW defects.

In this work, we consider planar pentaheptite graphene and we perform density functional calculations to investigate the effect of complete hydrogenation on the structural, energetics and electronic properties. The results are compared with pristine graphene and graphane. Given the isostructural nature of graphene and boronitrene, an analogous structure formed by reconstructing boronitrene into a periodic array of R_5 and R_7 rings, hereafter referred to as pentaheptite boronitrene, is also considered.

II. COMPUTATIONAL DETAILS

First principles calculations were performed within density functional theory (DFT) using the plane-wave self-consistent field (PWSCF) code included in the QUANTUM ESPRESSO distribution.[41] The projector augmented wave (PAW) potentials[42,43] were used to account for electron-ion interactions. Exchange and correlation energies were approximated by the Perdew, Burke, and Ernzerhof (PBE)[44] functional for the semi-local generalized gradient approximation (GGA). The one-electron pseudo-orbitals were expanded with a plane-wave kinetic energy cut-off of 500 eV.

For the structural optimizations, the Brillouin zone integrations were performed using a $6 \times 6 \times 1$ Monkhorst-Pack grid[45] of **k** points while a denser $12 \times 12 \times 1$ grid was used for the density of states calculations. The energy cut-off and **k** mesh were determined to be sufficient to produce well-converged energy differences for all structures. All the structures were optimized using the conjugate gradient method until the forces on all atoms were less than 0.01 eV/Å, and the total energy was converged to within within 10^{-7} eV. A large vacuum space of 15 Å was included perpendicular to the monolayer plane in order to avoid spurious interactions between the periodic images.

III. STRUCTURAL ASPECTS

The optimized pentaheptites structures that we considered are depicted in Fig. 1. Optimization was carried out with respect to both the atomic positions and rectangular cell parameters. Fig. 1(a) represents the pristine planar pentaheptite graphene, where four hexagonal (R_6) rings are transformed into two pentagon (R_5) and two heptagons (R_7) rings by the rotation of a C-dimer with respect to the midpoint of the bond as proposed by Crespi *et al.* (*cf.* Ref. 35). This implies that pentaheptites are generated

by simultaneous creation of SW-type defects over the entire graphene sheet, transforming pyrenelike rings into symmetrically paired pentagons and heptagons.[37,49] Although there are various ways in which the R_5 and R_7 rings can be constructed, it has been established that pentaheptites also adhere to the rule that the most favorable configurations are those which minimize the number of pentagon-pentagon pairs and maximize the number of pentagon-heptagon pairs, as is the case with *fullerenes* and *haeckelites* (*cf.* Refs. 36 and 37). Accordingly, this rule then leads to the requirement of a 16-atom rectangular conventional unit cell having a single pentagon-pentagon adjacency and multiple pentagon-heptagon adjacencies as seen on Fig. 1. The smallest repeating pentaheptite unit can be obtained from an 8-atom hexagonal primitive unit cell.

The selected optimized bond lengths (d_i) and angles (θ_i) denoted in the figures are shown in Table I. In comparison, the C-C bond lengths and angles in pristine graphene are uniform at 1.42 Å and 120° respectively. We notice a variation in bond lengths (1.39 Å to 1.49 Å) in pentaheptite graphene. The rotated C-C bonds (d_1 and d_8) are slightly compressed to 1.41 Å, whereas the first nearest bonds shared by adjacent pentagon and heptagon (i.e. d_2, d_4 and d_7) elongate to 1.49 Å. The C dimer d_6, shared by adjacent pentagon rings bears a compressive strain with a reduced bond length of 1.39 Å while adjacent heptagons share a bond length d_3 of 1.40 Å. Furthermore, it is noted that the bond angles in pentaheptite graphene deviate from the perfect hexagonal sp^2 bond angles of pristine graphene. For instance, the pentagonal angles (e.g. θ_1, θ_6 and θ_7) are reduced while the heptagonal angles (θ_3, θ_4, θ_8) increase, resulting in a more open structure.

	Bond distances				Bond angles		
Index	Graphene	Graphane	Boronitrene	Index	Graphene	Graphane	Boronitrene
d_1	1.41	1.54	1.40	θ_1	105.3	96.9	105.6
d_2	1.49	1.58	1.47	θ_2	127.4	117.0	129.3
d_3	1.40	1.51	1.72	θ_3	130.5	107.9	124.7
d_4	1.49	1.57	1.44	θ_4	139.2	128.1	132.0
d_5	1.40	1.52	1.42	θ_5	122.6	121.2	142.0
d_6	1.39	1.49	1.62	θ_6	107.0	96.4	102.8
d_7	1.49	1.60	1.38	θ_7	107.0	99.9	108.5
d_8	1.41	1.54	1.42	θ_8	127.4	122.1	119.5
d_9			1.39	θ_9			130.5

TABLE I: The optimized bond distances (d, in Å) and angles (θ, in degrees) for pentaheptite graphene, graphane and boronitrene derivatives as obtained by the PBE GGA functional. The indices d_i and θ_i denote the selected bond distances and angles respectively, as shown on Fig. 1.

Graphane (Ref. 15) is fully hydrogenated graphene with hydrogen absorbed at on-top sites alternately above and below the plane. Starting with graphane, we apply the repeated SW transformation described above where four R_6 rings are transformed into two R_5 and two R_7 rings by the rotation of a C-dimer with respect to the midpoint of the bond. This implies that pentaheptite graphane is generated by a simultaneous creation of SW-type defects over the entire graphane sheet, transforming hydrogenated pyrenelike rings into symmetrically paired hydrogenated pentagons and heptagons. Because of the odd-numbered rings, it should be obvious that there will now have to be two hydrogen atoms adjacent to each other on the R_5 and two R_7 rings. This results in a buckled structure as displayed in Fig. 1(b).

In comparison to the pristine pentaheptite graphene, we notice that all C-C bonds in the hydrogenated pentaheptite are further dilated, with the most elongation (0.13 Å) observed on the rotated bonds as denoted by (d_1). The C-C bond d_7 is the longest, at 1.60 Å, due to the adjacent H-H repulsion above the plane. The C-H bond length is found to be 1.10 Å, characteristic of covalent bonding as observed for graphane (Ref. 15) and other hydrocarbons. All the bond angles are reduced through buckling as the C atoms change towards sp^3 hybridization with the adsorbed H atoms. The scenario of adjacent H atoms below and above the plane is shown on Fig. 1(d). The adjacent H atoms below and above the plane are respectively 2.15 Å and 2.10 Å apart, while the C-H bond length remain the same at 1.10 Å.

Given the heteroelemental nature of boronitrene, the SW rotation of B-N bonds results in homoelemental B-B and N-N bonds as shown for the pentaheptite boronitrene in Fig. 1(c). The rotated B-N bonds, denoted d_1, bear a compressive strain to a bond length of 1.40 Å in comparison to a B-N bond length of 1.46 Å calculated for pristine boronitrene. The N-N (d_2) and B-B (d_3) bonds arising from the SW transformation are found to be 1.47 Å and 1.72 Å respectively. Generally, we notice a variation in B-N bond lengths from 1.38 Å (d_7) to 1.42 Å (d_4). As in the pristine pentaheptite graphene, the bond angles deviate from the constant value of 120° for pristine boronitrene, with pentagons having an average angle of 106°, and heptagons an average angle of 128.6°.

IV. RELATIVE STABILITY

Calculation of formation energies has become a common practice in first principles studies to evaluate the relative stabilities of materials and test their formation possibility. Since the formation of pentaheptites does not change the number of atoms,

we simply calculate the formation energy as the difference in equilibrium cohesive energy between the defected and parent structures, calculated at the same level of accuracy. For pentaheptite graphene and pristine graphene, the cohesive energies are found to be −7.51 eV/atom and −7.75 eV/atom, respectively. This implies that the energy of planar pentaheptite graphene is 0.24 eV/atom above a single layer of graphene. This result is comparable to a local density approximation energy difference of 0.33 eV/atom between the planar pentaheptite graphene and an isolated sheet of graphite as reported in Ref. 35. This relatively small positive value of formation energy means that this structure is, in principle, thermodynamically meta-stable (endothermic). It has been argued[35,46] that the energetic cost of rotating the entire bonds in planar pentaheptite graphene is slightly lower than the energy of C_{60} (Buckminsterfullerene), supporting the notion that pentaheptite graphene could be synthesizable.

For the hydrogenated pentaheptite graphene, we compute the formation energy with reference to the energies of monolayer graphene and diatomic hydrogen gas (H_2). Accordingly, we predict a positive formation energy of 0.06 eV/(CH pair), which is four times lower than that predicted for the pristine pentaheptite graphene. This reduction in formation energy is attributed to the hydrogen induced transformation from sp^2 bonding in the pristine graphene to sp^3 bonding in the hydrogenated structure. It is worth mentioning here that graphane is reported to be the most stable of the hydrocarbons with a C:H ratio of 1, such as benzene and acetylene.[15] For comparison purpose, we obtain at the same level of accuracy, a formation energy of −0.09 eV/(CH pair) for graphane chair, in good agreement with the result of Ref. 15. The energy difference between these two systems shows that the formation energy of pentaheptite graphane is 0.15 eV/atom above that of pristine chairlike graphane. Like in the boat conformer of graphane, it is expected that repulsion of the two adjacent H atoms bonded to the nearest neighbor carbon atoms could also have an effect on the formation possibility of the hydrogenated pentaheptite graphene. However, the positive formation energies for the pentaheptites do not necessarily rule out the possibility to synthesize them. The physical conditions assumed for static DFT calculations (i.e. zero temperature and pressure) may also contribute towards the positive energy values.

In the case of pentaheptite boronitrene, taking the difference between its equilibrium cohesive energy (−11.49 eV/(BN pair)) and that of pristine boronitrene (−13.33 eV/(BN pair) results in the formation energy of 1.84 eV/BN pair. When comparing the formation energies for the two pentaheptites, we deduce that the rotation of B-N bonds requires more energy due to the formation of unfavorable homoelemental (B-B and N-N) bonds, as opposed to the rotation of C-C bonds. Even though the SW defects in monolayer *h*-BN are predicted by various theoretical studies,[19,47] they have never been found experimentally (*cf.* Ref. 48).

V. ELECTRONIC PROPERTIES

In order to understand the effects of bond rotations on the electronic structure, we analyze the band structures and density of states (DOS) for the considered pentaheptite systems as shown in Figs. 2 and 3. For the purpose of comparison with the pentaheptite boronitrene, we also show the band structure and DOS for the pristine boronitrene system based on a rectangular lattice.

The band structure of pristine planar pentaheptite graphene is shown in Fig. 2(a). Unlike in pristine graphene, this band structure exhibits a clear metallic behavior with a substantial Fermi surface around the Γ point, in agreement with the earlier tight-binding band structure as reported by Crespi *et al.* (Ref. 35). The highly dispersive π and π^* bands randomly cross the Fermi level along the $X - \Gamma - Y$ path, closing the pseudo-gap at the Fermi level of graphene. This metalization is also evident in the corresponding DOS plot as displayed in Fig. 2(b), which yields a DOS of 2.10 states per eV per cell at the Fermi energy. This is equivalent to 0.13 state per eV per C atom, in agreement with 0.1 state per eV per C atom obtained in Ref 35.

The interesting result, however, is the electronic structure associated with adsorption of atomic hydrogen on the entire pentaheptite graphene sheet. Figs. 2(c) and (d) show respectively, the band structure and the corresponding DOS plots for the fully hydrogenated pentaheptite graphene. We find that the effect of hydrogenation on the entire pentaheptite graphene is to open a wide direct band gap of 3.78 eV at the Y point. In contrast to the planar pentaheptite graphene, H adsorption changes the C atoms from sp^2 to sp^3 hybridization as already discussed in section III. Consequently, the π and π^* bonds vanish, giving rise to almost flat bands in the upper valence and lower conduction regions. We suggest that this band gap can possibly be tuned by systematically adjusting the density of hydrogen atoms from low towards full coverage.

To gain insight into the electronic structure of pentaheptite boronitrene, we begin by examining the pristine boronitrene monolayer system whose calculated band structure and DOS are displayed in Fig. 3(a) and (b). It is well known that boronitrene is an insulating material. Our calculation yields a direct band gap of 4.36 eV, in good agreement with 4.53 eV reported in Ref. 34. On transforming the structure to a pentaheptite of boronitrene (Fig. 3(c) and (d)), we notice a remarkable reduction in band gap, turning the system into a semiconductor with a direct band gap of 0.71 eV at the Γ point.

VI. CONCLUSIONS

We studied pentaheptite graphene, graphane and boronitrene derivatives using density functional methods within the GGA. We conclude that pentaheptite graphene is a metal with an energy of 0.24 eV/atom above pristine graphene. Pentaheptite graphane is more stable at 0.15 eV/(CH pair) above graphane, and is insulating in nature with a bandgap of 3.78 eV. Hydrogenation induces

sp^2 to sp^3 hybridization which is responsible for stablizing this system. Pentaheptite boronitrene is 1.84 eV/(BN pair) above pristine boronitrene. There is a marked reduction in the bandgap from 4.36 eV to 0.71 eV at the Γ point.

ACKNOWLEDGMENTS

We thank the National Research Foundation (NRF) and University of Pretoria for financial support, and Dr Jannie Pretorius and Prof Walter Meyer for help with the use of the computational resources. NC is thankful to the National Institute for Theoretical Physics for support.

* Mahlaga.Molepo@up.ac.za

[1] K. S. Novoselov, A. K. Geim, S. V. Morozov, D. Jiang, Y. Zhang, S. V. Dubonos, I. V. Grigorieva, and A. A. Firsov, Science **306**, 666 (2004).
[2] A. H. Castro Neto, F. Guinea, N. M. R. Peres, K. S. Novoselov, and A. K. Geim, Rev. Mod. Phys. **81**, 109 (2009).
[3] P. Avouris, Z. Chen, and V. Perebeinos, Nat. Nanotech. **2**, 605 (2007).
[4] A. K. Geim and K. S. Novoselov, Nat. Mater. **6**, 183 (2007).
[5] H. Sachdev, F. Müller, and S. Hüfner, Diamond Relat. Mater. **19**, 1027 (2010).
[6] K. S. Novoselov, D. Jiang, F. Schedin, T. Booth, V. V. Khotkevich, S. Morozov, and A. K. Geim, Proc. Natl. Acad. Sci. U.S.A. **102**, 10451 (2005).
[7] J. A. Yan, L. Xian, and M. Y. Chou, Phys. Rev. Lett. **103**, 086802 (2009).
[8] Z. Luo, P. M. Vora, E. J. Mele, A. T. C. Johnson, and J. M. Kikkawa, Appl. Phys. Lett. **94**, 111909 (2009).
[9] D. C. Elias, R. R. Nair, T. M. G. Mohiuddin, S. V. Morozov, P. Blake, M. P. Halsall, A. C. Ferrari, D. W. Boukhvalov, M. I. Katsnelson, A. K. Geim, and K. S. Novoselov, Science **323**, 610 (2009).
[10] I. Zanella, S. Guerini, S. B. Fagan, J. Mendes Filho, and A. G. Souza Filho, Phys. Rev. B **77**, 073404 (2008).
[11] D. W. Boukhvalov, M. I. Katsnelson, and A. I. Lichtenstein, Phys. Rev. B **77**, 035427 (2008).
[12] D. W. Boukhvalov and M. I. Katsnelson, Phys. Rev. B **78**, 085413 (2008).
[13] R. M. Ribeiro, N. M. R. Peres, J. Coutinho, and P. R. Briddon, Phys. Rev. B **78**, 075442 (2008).
[14] S. Lebegue, M. Klintenberg, O. Eriksson, and M. I. Katsnelson, Phys. Rev. B **79**, 245117 (2009).
[15] J. O. Sofo, A. S. Chaudhari, and G. D. Barber, Phys. Rev. B **75**, 153401 (2007).
[16] M. T. Lusk and L. D. Carr, Phys. Rev. Lett. **100**, 175503 (2008).
[17] M. T. Lusk and L. D. Carr, Carbon **47**, 2226 (2009).
[18] S. C. Pradhan and J. K. Phadikar, Phys. Lett. A **373**, 1062 (2009).
[19] J. Ma, D. Alfe, A. Michaelides, and E. Wang, Phys. Rev. B **80**, 033407 (2009).
[20] L. D. Carr and M. T. Lusk, Nat. Nanotech. **5**, 316 (2010).
[21] F. Banhart, J. Kotakoski, and A. V. Krasheninnikov, ACS Nano **5**, 26 (2011).
[22] D. J. Appelhans, Z. Lin, and M. T Lusk, Phys. Rev. B **82**, 073410 (2010).
[23] D. J. Appelhans, L. D. Carr, and M. T. Lusk, New J. Phys. **12**, 125006 (2010).
[24] L. Brey and H. A Fertig, Phys. Rev. B **73**, 235411 (2006).
[25] O. Hod, V. Barone, J. E. Peralta, and G. E. Scuseria, Nano Lett. **7**, 2295 (2007).
[26] E. R. Mucciolo, A. H. Castro Neto, and C. H. Lwenkopf, Phys. Rev. B **79**, 075407 (2009).
[27] S. Bhandary, O. Eriksson, B. Sanyal, and M. I. Katsnelson, Phys. Rev. B **82**, 165405 (2010).
[28] J. Bai, X. Zhong, S. Jiang, Y. Huang, and X. Duan, Nat. Nano-technol. **5**, 190 (2010).
[29] A. J. Stone and D. J. Wales, Chem. Phys. Lett. **128**, 501 (1986).
[30] M. Buongiorno Nardelli, B. I. Yakobson, and J. Bernholc, Phys. Rev. Lett. **81**, 4656 (1998).
[31] M. Buongiorno Nardelli, B. I. Yakobson, and J. Bernholc, Phys. Rev. B **57**, R4277 (1998).
[32] G. G. Samsonidze, G. G. Samsonidze, and B. I. Yakobson, Phys. Rev. Lett. **88**, 065501 (2002).
[33] C. P. Ewels, M. I. Heggie, and P. R. Briddon, Chem. Phys. Lett. **351**, 178 (2002).
[34] P. P. Shinde and V. Kumar, Phys. Rev. B **84** 125401 (2011).
[35] V. H. Crespi, L. X. Benedict, M. L. Cohen, and S. G. Louie, Phys. Rev. B **53** R13303 (1996).
[36] E. Albertazzi, C. Domene, P. W. Fowler, T. Heine, G. Seifert, C. Van Alsenoyd and F. Zerbettoe, Phys. Chem. Chem. Phys. **1**, 2913 (1999).
[37] H. Terrones, M. Terrones, E. Hernandez, N. Grobert, J-C. Charlier, and P. M. Ajayan, Phys. Rev. Lett. **84**, 1716 (2000).
[38] D. Malko, C. Neiss, F. Vines, and A. Gorling, Phys. Rev. Lett. **108**, 086804 (2012).
[39] L. Chen, J. Li, D. Li, M. Wei, and X. Wang, Solid. State Commun. **152**, 1985 (2012).
[40] E. J. Duplock, M. Scheffler, and P. J. D. Lindan, Phys. Rev. Lett. **92**, 225502 (2004).
[41] P. Giannozzi, S. Baroni, N. Bonini, M. Calandra, R. Car, C. Cavazzoni, D. Ceresoli, G. L. Chiarotti, M. Cococcioni, I. Dabo, A. Dal Corso, S. Fabris, G. Gougoussis, A. Kokalj, M. Lazzeri, L. Martin-Samos, N. Marzari, F. Mauri, R. Mazzarello, S. Paolini, A. Pasquarello, L. Paulatto, C. Sbraccia, S. Scandolo, G. Sclauzero, A. P. Seitsonen, A. Smogunov, P. Umari, and R. M. Wentzcovitch, J. Phys. Condens. Matter **21**, 395502 (2009).
[42] P. E. Blochl, Phys. Rev. B **50**, 17953 (1994).
[43] G. Kresse and D. Joubert, Phys. Rev. B **59**, 1758 (1999).
[44] J. P. Perdew, K. Burke, and M. Ernzerhof, Phys. Rev. Lett. **77**, 3865 (1996).
[45] H. J. Monkhorst and J. D. Pack, Phys. Rev. B **13**, 5188 (1976).
[46] V. H. Crespi and M. L. Cohen, Phys. Rev. Lett. **79**, 2093 (1997).
[47] G. J. Slotman and A. Fasolino, J. Phys.: Condens. Matter **25**, 045009 (2013).
[48] C. Jin, F. Lin, K. Suenaga, and S. Iijima1, Phys. Rev. Lett. **102**, 195505 (2009).
[49] M. Deza, P. W. Fowler, M. Shtogrin. and K. Vietze, J. Chem. Inf. Comput. Sci. **40**, 1325 (2000).

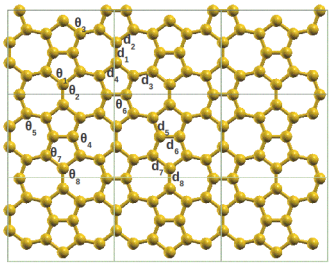

(a)

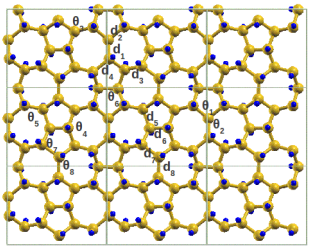

(b)

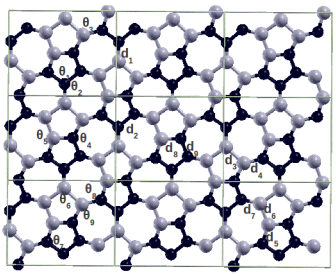

(c)

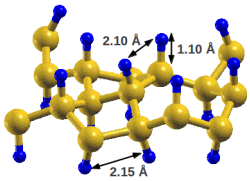

(d)

FIG. 1: (Color online) Optimized atomic structures for (a) pentaheptite graphene, (b) pentaheptite graphane, and (c) pentaheptite boronitrene. The gold, blue, black, and gray colored balls represent C, H, N, and B atoms, respectively. The magnitudes of the labeled bond distances d_i and angles θ_i are displayed on table I. (d) shows the adjacent H atoms in pentaheptite graphane, below and above the plane.

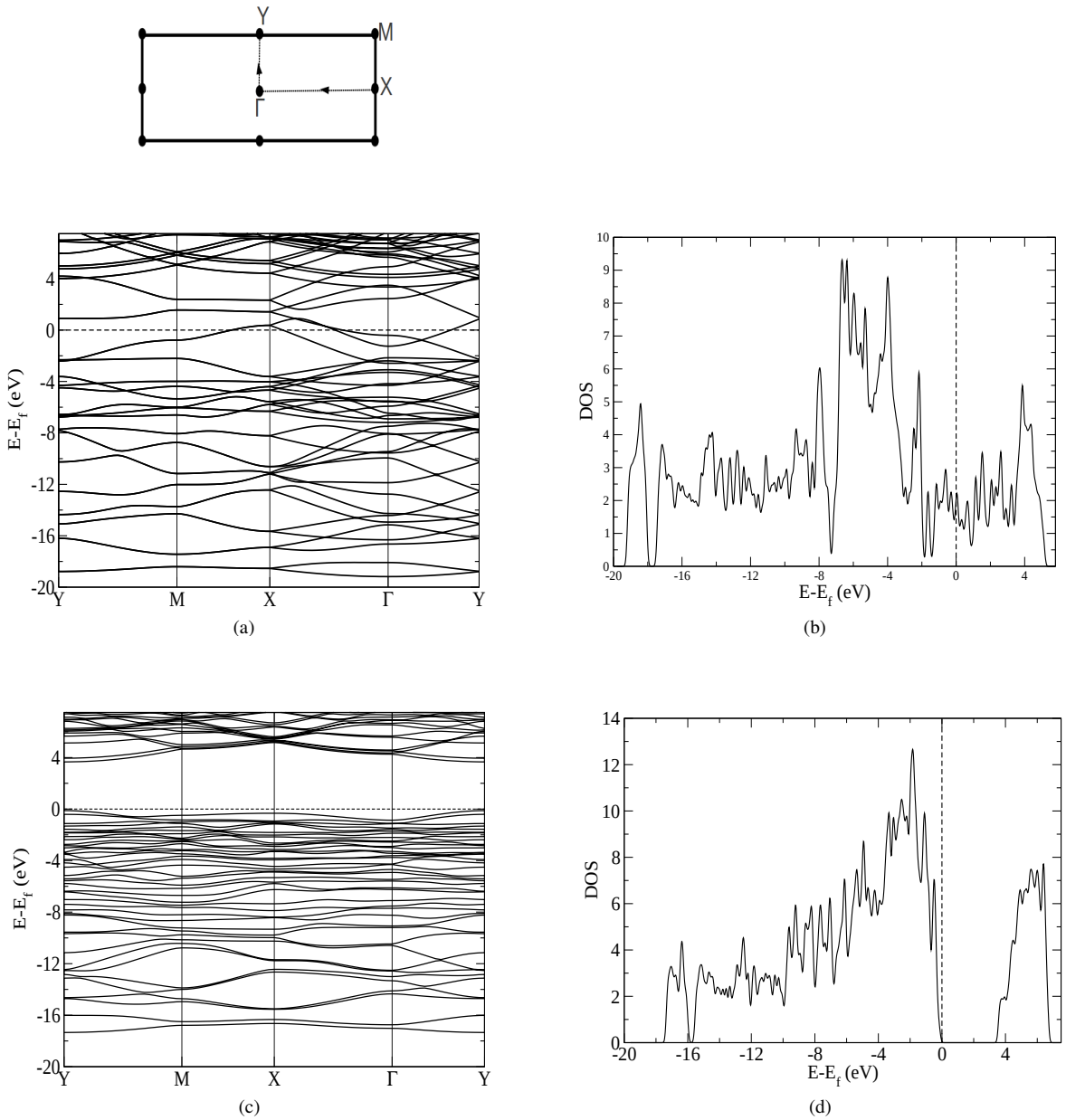

FIG. 2: The electronic band structure (left panel) and corresponding density of states (DOS) (right panel) for [(a)-(b)] a periodic sheet of pristine pentaheptite graphene and [(c)-(d)] hydrogenated pentaheptite graphene. The bands are plotted along a high symmetry path of the rectangular Brillouin zone shown at the top. The Fermi energy E_f, is set at zero, marked by the dotted line. A band gap $E_g = 3.78$ eV is induced by hydrogenation.

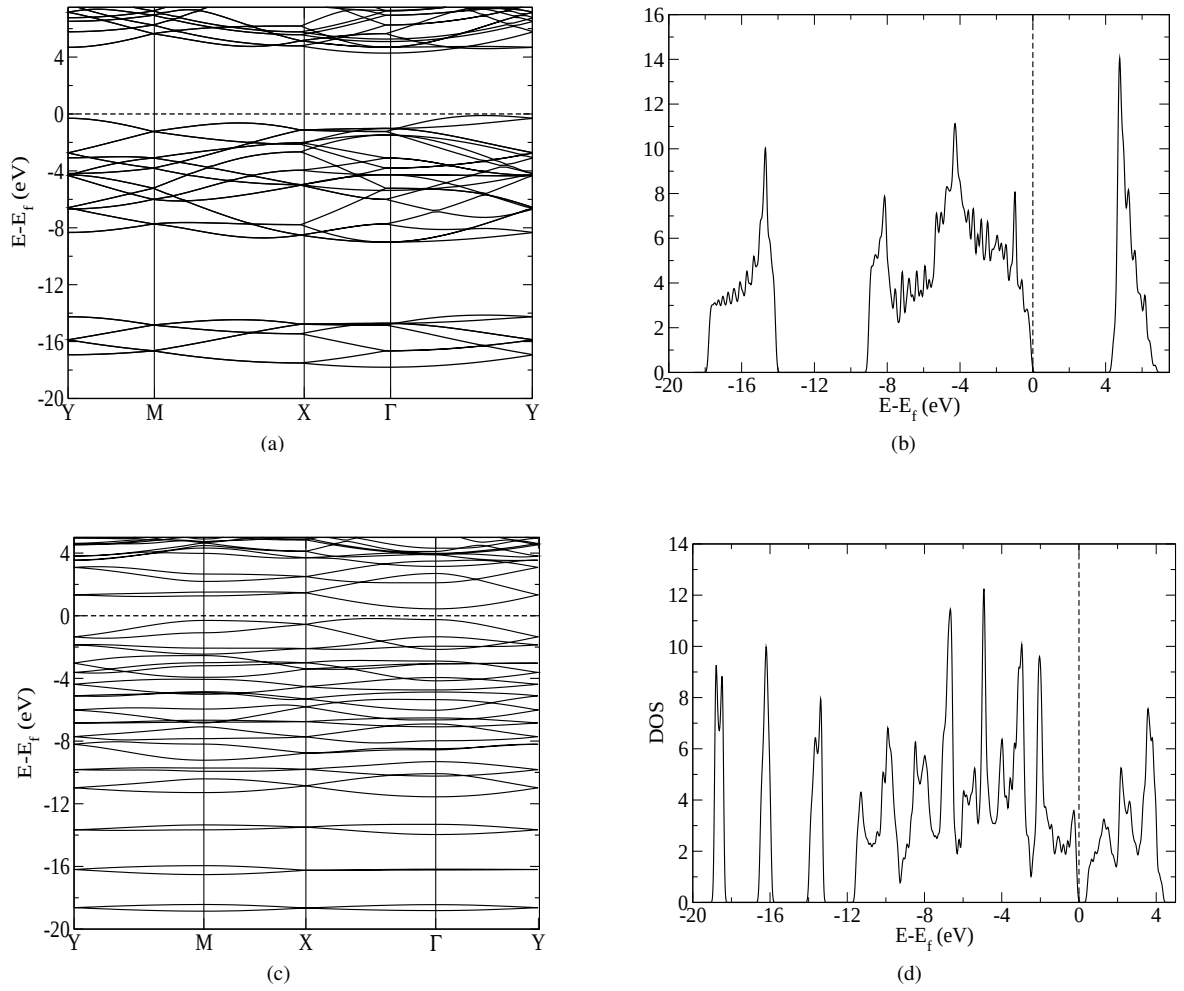

FIG. 3: The electronic band structure (left panel) and corresponding density of states (DOS) (right panel) of [(a)-(b)] pristine boronitrene (*h*-BN) and [(c)-(d)] pentaheptite boronitrene. The bands are plotted along the same high symmetry path as in Fig. 2. The Fermi energy E_f, is set at zero, marked by the dotted line. A band gap E_g is reduced from 4.36 eV to 0.71 eV.